Chapter 2
Rotordynamic Analysis of the Turbopump Using Superelement Approach

Yunus Ozcelik, Hakan Bayraktar, and Yunus Tufek

Abstract The use of turbopumps in aerospace propulsion systems and high-performance fluid transport applications necessitates thorough rotordynamic analysis to ensure efficiency and reliability. The complexity of turbopumps, with factors like high speeds, fluid-structure interactions, and flexible components, requires advanced modeling techniques for accurate predictions. Model reduction techniques like Component Mode Synthesis (CMS) are crucial for efficient dynamic analysis of complex systems. This study analyzed the rotordynamic behavior of the turbopump using a superelement approach. The rotor was modeled using 3D elements in ANSYS, with its dynamic characteristics evaluated under constant bearing stiffness. To enhance computational efficiency, the stator was represented as a superelement and coupled with the 3D rotor model. For validation, a full 3D stator model was also developed and coupled with the rotor. This comprehensive modeling strategy enabled a detailed assessment of the system's dynamic behavior. Results validated against the full rotor–stator model demonstrated that stator flexibility has a notable effect on the rotor's critical speeds. The study highlights the effectiveness of the superelement method in reducing computational costs while maintaining the accuracy required for high-fidelity rotordynamic analysis.

Keywords Rotordynamic · Turbopump · Component Mode Synthesis · Superelement

Introduction

Turbopumps are critical subsystems in aerospace propulsion systems, commonly used in liquid rocket engines and other high-performance fluid transport applications. They consist of a pump driven by a turbine, which operates at extremely high rotational speeds to deliver the required power. Due to the high operating speeds and complex structural interactions, turbopumps are subject to various dynamic phenomena that can significantly affect their performance and reliability.

One of the most crucial aspects of turbopump design and analysis is rotordynamic, which examines the dynamic behavior of the rotating components, including the rotors, bearings, seals, and the surrounding casings. Rotordynamic analysis is essential for predicting critical speeds, stability margins, and potential failure modes such as rotor whirl and resonance, which can lead to excessive vibrations and mechanical failure. A thorough understanding and optimization of turbopump rotordynamic behavior are key to ensuring efficient, stable, and reliable operation under a wide range of operating conditions.

The high rotational speeds of turbopumps, coupled with the presence of fluid-structure interactions, bearings, seals, and flexible stator components, contribute to the complexity of their rotordynamic analysis. Factors such as rotor flexibility, bearing stiffness, and damping characteristics, as well as seal forces and casing flexibility, all play a role in determining the system's dynamic response. Identifying and addressing rotordynamic issues early in the design phase is crucial to avoiding costly failures and ensuring smooth operation throughout the entire operating range.

A rotor system must be designed to operate without excessive vibration throughout its entire speed range. The theoretical foundation of rotordynamic analysis dates to the late 18th century when Dunkerly [1] proposed that the critical speed of a rotor corresponds to the natural frequency of a simply supported beam. Early design approaches assumed rigid bearings. However, as operating speeds increased and computational methods advanced, rotor dynamics analysis evolved to account for bearing properties. It is well-established that the structure beyond the bearings, known as the foundation, tends to reduce

Yunus Ozcelik · Hakan Bayraktar · Yunus Tufek
Roketsan Inc.
e-mail: yunuseozcelik@gmail.com; hakan.bayraktar@roketsan.com.tr; yunus.tufek@roketsan.com.tr

Matthew Allen et al. (eds.), *Special Topics in Structural Dynamics & Experimental Techniques, Vol. 5*, Conference Proceedings of the Society for Experimental Mechanics Series, https://doi.org/10.13052/97887-438-0150-4_2

the first critical speed frequency while increasing the amplification factor [2]. These studies demonstrate that considering both bearing and foundation effects in rotor dynamics analysis leads more accurate rotor dynamics predictions.

Rotordynamic analysis using one-dimensional (1D) elements, where the shaft is represented by beam or bar elements and the disks are idealized as a concentrated mass, is widely employed in industry due to its simplicity and computational efficiency [3]. However, this approach has notable limitations, particularly in its inability to model complex rotor geometries or accurately capture the effects of large flexible disks and blades. For axisymmetric rotors, two-dimensional (2D) axisymmetric harmonic elements can be used, as they consider the three-dimensional (3D) nature of the problem while reducing the number of elements needed for modeling [4].

With advancements in modeling, analysis, optimization techniques, and material science, modern rotor configurations frequently incorporate non-uniform shaft diameters, hollow components, and large flexible structures. These features necessitate more sophisticated modeling techniques to accurately predict their dynamic behavior. 2D axisymmetric harmonic elements are insufficient for representing complex, non-uniform rotor blade geometries. This limitation has led to the increased use of 3D solid and shell elements, which offer a more accurate and geometrically complete representation of the rotor. These elements allow for analysis in both the fixed and rotating reference frames, reducing the need for geometric simplifications that remain prevalent in industrial practice.

Modeling rotors with 3D shell and solid elements offers the advantage of accurately representing complex rotor geometries. However, 3D rotor models are more suitable for analysis in the rotating reference frame and tend to result in significantly larger problem sizes [5]. Despite advancements in computational resources, linear rotordynamic analyses can still take hours or even days to complete [6]. To integrate such models into the commercial engineering design of critical components, and to account for nonlinear effects from bearings and dampers, it is crucial to improve dynamic analysis performance by orders of magnitude. Crucially, this improvement must be achieved without sacrificing model complexity or solution accuracy.

The application increase in model size for rotors modeled with 3D elements necessitates the use of model reduction techniques. Component Mode Synthesis (CMS) is a model reduction technique that allows for the efficient dynamic analysis of large and complex mechanical systems by breaking them down into smaller, manageable substructures. These substructures are individually analyzed, and their dynamic properties (e.g., mass, stiffness, and damping) are characterized through modal parameters such as natural frequencies and mode shapes. CMS enables the recombination of these modes to form a reduced-order model for the entire system, significantly decreasing the computational load while preserving the essential dynamic characteristics.

The use of CMS to reduce the computational effort for analyzing large rotating machinery, particularly in turbochargers, has been demonstrated by Kim et al. [7], while maintaining accuracy in predicting critical speeds and response amplitudes. CMS methods have also been applied to analyze the dynamic behavior of rotor-bearing systems under unbalance forces, enabling the inclusion of nonlinear effects like bearing stiffness and damping [3]. CMS was employed to investigate the dynamics of a turbopump rotor system in a study conducted by Lund [8]. The research highlighted the method's ability to predict natural frequencies and mode shapes accurately, facilitating the identification of critical speeds that could lead to resonance. Similarly, the superelement method has been used in the design optimization of rotor-bearing systems to predict how component modifications would affect overall system behavior, as shown in a study by Ehrich [9]. The combination of CMS with nonlinear effects has been gaining traction in recent years. CMS with nonlinear rotordynamic phenomena, such as oil whip and shaft bending, was integrated, demonstrating the method's versatility in capturing complex real-world dynamics that are difficult to handle with traditional full-order models, by Gupta et al. [10].

In this study, the rotordynamic behavior of a turbopump, including both the rotor and stator, was investigated using a combination of 3D modeling and superelement techniques obtained through the CMS method. The rotor was initially modeled with 3D finite elements in ANSYS, and its dynamic characteristics were evaluated under the assumption of constant bearing stiffness. To further enhance the analysis, the rotor was coupled with a stator represented as a condensed superelement, simplifying the stator's influence on the rotordynamic. Furthermore, a full 3D model of the stator was created in ANSYS and coupled with the rotor to validate the reduced model. This detailed approach provided an in-depth analysis of how the interaction between the rotor and stator influences the critical speeds of the turbopump.

Background

Substructuring is a technique that condenses a group of finite elements into a single equivalent element, represented by a reduced-order matrix. This condensed element is referred to as a superelement. In analytical procedures, a superelement is treated comparably to any other element type, with the exception that it necessitates an initial substructure generation analysis for its creation. Substructuring significantly reduces computational effort and solution time of large-scale problems while reducing the requirement for computational resources. This method proves particularly beneficial in nonlinear analyses and in examinations involving structures with recurring geometric configurations, such as rotordynamic analysis. In nonlinear analysis, substructuring can be implemented in the linear sections of the model, thereby eliminating the necessity for repetitive recalculation of element matrices during each equilibrium iteration. For structures characterized by repetitive patterns, a singular superelement can be generated to represent the recurring geometry and replicated across various locations, resulting in substantial savings in computational time.

In substructuring analysis, the nodal displacement vector $\{u\}$ of a substructure is expressed in terms of reduced coordinates $\{\hat{u}\}$, by following transformation [11]

$$\{u\} = [T]\,\{\hat{u}\}, \tag{1}$$

where $[T]$ is the transformation matrix.

In dynamic analysis, equation of motion can be expressed by,

$$[M]\,\{\ddot{u}\} + [C]\,\{\dot{u}\} + [K]\,\{u\} = \{F\}, \tag{2}$$

where $[M]$, $[C]$ and $[K]$ are mass, damping and stiffness matrix, respectively and $\{F\}$ is the load vector.

By substituting Eq. (1) into Eq. (2) and left multiplying by $[T]^T$, the following reduced equation is obtained,

$$\left[\hat{M}\right]\{\ddot{\hat{u}}\} + \left[\hat{C}\right]\{\dot{\hat{u}}\} + \left[\hat{K}\right]\{\hat{u}\} = \{\hat{F}\} \tag{3}$$

where, $\left[\hat{M}\right] = [T]^T\,[M]\,[T]$ is the reduced mass matrix, $\left[\hat{C}\right] = [T]^T\,[C]\,[T]$ is the reduced damping matrix, $\left[\hat{K}\right] = [T]^T\,[K]\,[T]$ is the reduced stiffness matrix and $\{\hat{F}\} = [T]^T\{F\}$ is the reduced load vector.

Static condensation, often referred to as Guyan Reduction, and Component Mode Synthesis (CMS) are both widely used techniques for substructuring in structural dynamics. Guyan Reduction is typically insufficient to fully capture the dynamic behavior of a superelement. To address this, static condensation is enhanced with the inclusion of component modes and residual vectors. When applying CMS to reduce a complex engineering model, certain loading conditions may induce deformation states that cannot be accurately represented by static reduction and component modes alone. In such cases, the Residual Vector technique is used to incorporate high-frequency contributions, compensating for this deformation discrepancy and ensuring an accurate dynamic response across all loading conditions. In this study, CMS is utilized to model the stator component of the turbopump. By applying equilibrium and compatibility conditions at the component interfaces, the method defines the dynamic behavior of the entire system model.

Dividing the matrix equation into degrees of freedom (DOFs) for the interface and interior,

$$\begin{aligned} &\{u\} = \begin{Bmatrix} \{u_m\} \\ \{u_c\} \end{Bmatrix}, \quad [M] = \begin{bmatrix} [M_{mm}] & [M_{mc}] \\ [M_{cm}] & [M_{cc}] \end{bmatrix}, \quad [C] = \begin{bmatrix} [C_{mm}] & [C_{mc}] \\ [C_{cm}] & [C_{cc}] \end{bmatrix}, \\ &[K] = \begin{bmatrix} [K_{mm}] & [K_{mc}] \\ [K_{cm}] & [K_{cc}] \end{bmatrix}, \quad \{F\} = \begin{Bmatrix} \{F_m\} \\ \{F_c\} \end{Bmatrix} \end{aligned} \tag{4}$$

where, m is the master DOF that defined at interference, and c is all nodes except master nodes.

Nodal displacement vector can be expressed by,

$$\{u\} = \begin{Bmatrix} \{u_m\} \\ \{u_c\} \end{Bmatrix} = [T] \begin{Bmatrix} \{u_m\} \\ \{y_\delta\} \end{Bmatrix} \tag{5}$$

where, $\{y_\delta\}$ is a truncated set of generalized modal coordinates. Transformation matrix used in this study is obtained by [12],

$$[T] = \begin{bmatrix} [I] & [0] \\ [G_{cm}] & [\Phi_c] \end{bmatrix} \tag{6}$$

where, $[\Phi_c]$ is the eigenvector obtained with interference nodes fixed.

In the reduced system, master DOFs serve to connect the CMS superelement with other elements or additional CMS superelements.

For the fixed-interface method, when the fixed-interface normal modes are mass-normalized, the resulting reduced stiffness, mass, and damping matrices, as well as the reduced load vector, take the following final form [13]:

$$[\hat{M}] = \begin{bmatrix} [M_{mm}] + [M_{mc}]\,[G_{cm}] + [G_{mc}]\,[[M_{cm}] + [M_{cc}]\,[G_{cm}]] & [[M_{mc}] + [G_{mc}]\,[M_{cc}]\,[[\Phi_c] \\ [\Phi_c]^T\,[[M_{cm}] + [M_{cc}]\,[G_{cm}]] & [I] \end{bmatrix} \tag{7}$$

$$[\hat{C}] = \begin{bmatrix} [C_{mm}] + [C_{mc}]\,[G_{cm}] + [G_{mc}]\,[[C_{cm}] + [C_{cc}]\,[G_{cm}]] & [[C_{mc}] + [G_{mc}]\,[C_{cc}]]\,[\Phi_c] \\ [\Phi_c]^T\,[[C_{cm}] + [C_{cc}]\,[G_{cm}]] & [\Phi_c]^T\,[C_{cc}]\,[\Phi_c] \end{bmatrix} \tag{8}$$

$$[\hat{K}] = \begin{bmatrix} [K_{mm}] + [K_{mc}][G_{cm}] & [0] \\ [0] & [\Lambda^2] \end{bmatrix} \tag{9}$$

$$\{\hat{F}\} = \begin{Bmatrix} \{F_m\} + [G_{mc}]\,\{F_c\} \\ [\Phi_c]^T\,\{F_c\} \end{Bmatrix} \tag{10}$$

where, $[G_{cm}] = -[K_{cc}]^{-1}\,[K_{cm}]$, $[G_{mc}] = [G_{cm}]^{-T}$ and , $[\Lambda^2]$ is a diagonal matrix consisting of the eigenvalues of the retained fixed-interface normal modes.

The displacements at the condensed or DOFs are obtained from Eq. (5). For the fixed-interface condition, they are computed using Craig-Bampton method as follows:

$$\{u_c\} = [G_{cm}]\,\{u_m\} + [\phi_c]\,\{y_\delta\} \tag{11}$$

In rotordynamic analysis, the dynamic equation in a stationary reference frame can be expressed as:

$$[M]\,\{\ddot{u}\} + ([G] + [C])\{\dot{u}\} + ([B] + [K])\{u\} = \{F\}, \tag{12}$$

where, [G] is the gyroscopic matrix which plays a critical role in rotordynamic analysis as it depends on the rotational velocity and, [B] is the rotating damping matrix.

When a structure rotates about an axis such as Z and a precession motion (a rotation about an axis perpendicular to Z Axis) is introduced, a reaction moment arises. This reaction, known as the gyroscopic moment, acts along an axis that is perpendicular to both the spin axis Z and the precession axis. The gyroscopic matrix [G] represents this effect by coupling degrees of freedom in planes that are perpendicular to the spin axis in finite element modeling. Notably, this matrix is skew-symmetric, reflecting the nature of gyroscopic forces.

Whirling refers to the circular or elliptical motion exhibited by a rotating structure when it vibrates at its resonant frequency. This motion can occur in two distinct forms: forward whirl (FW), which occurs when the motion is in the same direction as the rotational velocity, and backward whirl (BW), which takes place when the motion opposes the direction of rotation. Both forms of whirling are critical in understanding the dynamic behavior of rotating systems, as they can influence stability and performance, particularly at resonance.

The critical speed refers to the rotational speed at which a structure's resonance frequency (or frequencies) coincides with the excitation frequency. This condition arises when the natural frequency of the system matches the frequency of the applied excitation, which can result from an unbalance that is synchronous with the rotational speed. To identify critical speeds, one effective approach is to conduct a Campbell diagram analysis. This involves calculating the intersection points between the frequency curves and the excitation line, which reveal the critical speeds of the system. This study focuses exclusively on the effect of unbalance forces synchronous with the rotational speed.

Methodology

In this study, the rotordynamic behavior of a turbopump, including the stator, was analyzed using a superelement approach. The rotor was modeled using 3D elements in ANSYS, and its dynamic characteristics were evaluated under the assumption of constant bearing stiffness. Subsequently, the rotor model was coupled with a superelement representing the entire stator. Additionally, the rotor was connected to the full stator model, which was also constructed using 3D elements in ANSYS, allowing for a comprehensive analysis of the system's dynamic performance.

Rotordynamic Model with Fixed Bearing Stiffness

A simplified model of the turbopump rotor, excluding the casing, was created using constant stiffness properties. Figure 1 illustrates a rotor configuration for the analysis, showing several rotating components arranged sequentially from the left end of the shaft: nut, front inducer, front impeller, front bearing and rear inducer, rear impeller, rear bearing and turbine. Additionally, the lumped mass model of the rotating non-axisymmetric components, such as blades of impeller, inducer and turbine are also represented in Figure 1. Since the objective of this study is to evaluate the impact of using a superelement on solution time and accuracy, the stiffness and damping effects of the seals are excluded from the scope of the analysis.

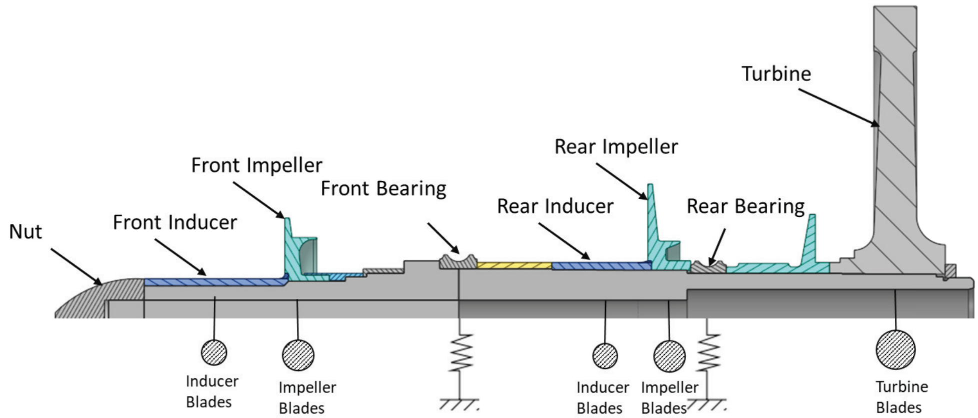

Fig. 1 The Turbopump Rotor Configuration.

The turbopump, powered by a turbine using hot, high-pressure gas, operates at a rotational speed of 23,500 RPM under steady-state conditions. It is assumed that both the front and rear bearings are isotropic with a stiffness of 10^8 N/mm. Inconel 718 superalloy, with a density of 8240 kg/m^3, a Young's modulus of 200 GPa, and a Poisson's ratio of 0.3, was assigned to rotor components. As illustrated in Figure 2, the rotor model was discretized with 105,344 SOLID185 elements, which are first-order hexahedral elements in ANSYS. Bonded contacts were employed at all component interfaces to simulate interference. Additionally, COMBI214 elements were utilized to represent the bearings within the model.

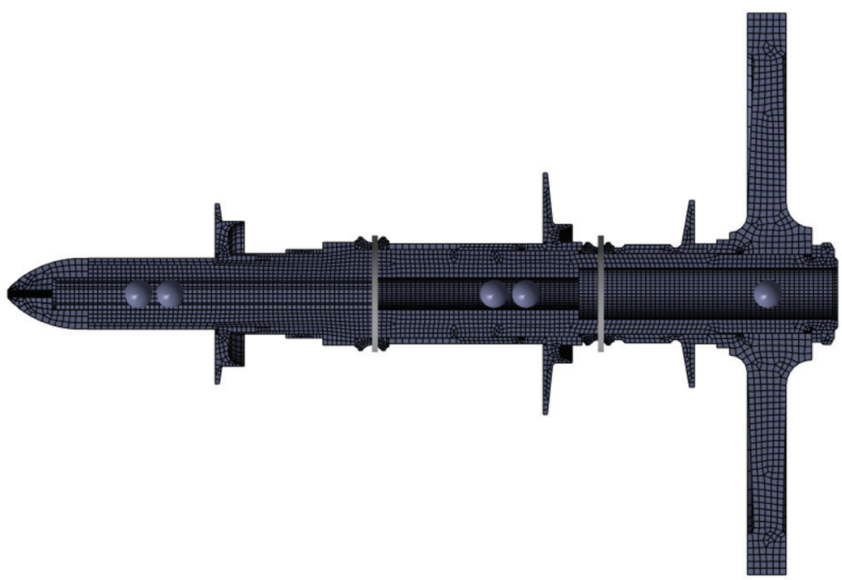

Fig. 2 Cross-sectional View of the 3D Finite Element Model of the Turbopump Rotor.

A complex eigenvalue analysis was conducted to generate the Campbell diagram over a range of rotor speeds (5,000-30,000 RPM), as shown in Figure 3. In this diagram, the 1X line denotes the rotor's operating speed. Figure 4 illustrates the first backward (1st BW) and first forward (1st FW) mode shapes of the rotor when operating at a speed of 5,000 RPM. These mode shapes provide insight into the rotor's dynamic behavior under these conditions. The overhang configuration of the turbine, along with its large diameter and mass, causes the first bending mode to predominantly involve shaft deflection on the turbine side, while the other rotor components remain largely unaffected and stationary.

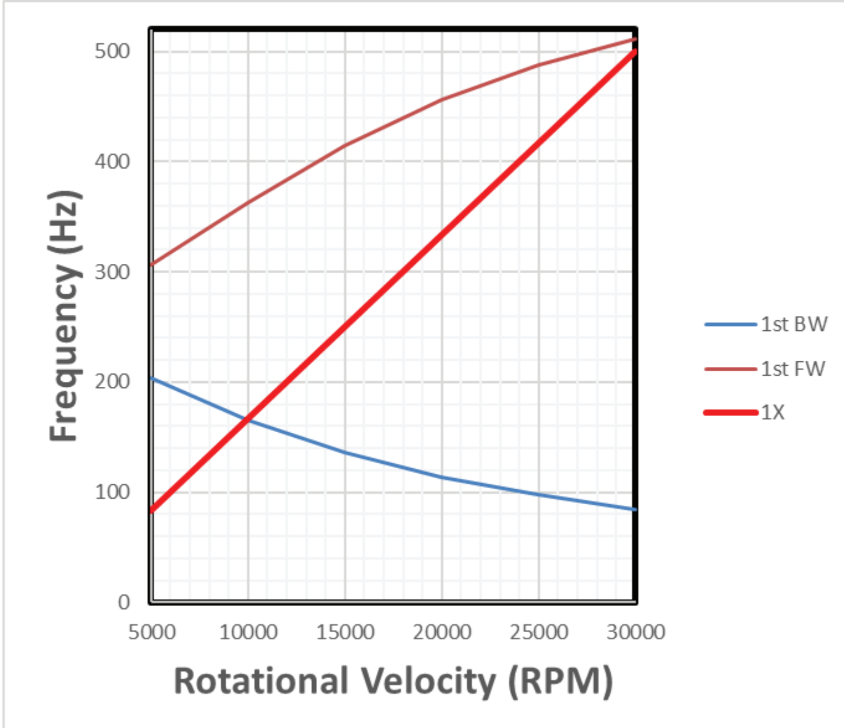

Fig. 3 Campbell Diagram of the Turbopump Rotor with Fixed Bearing Stiffness.

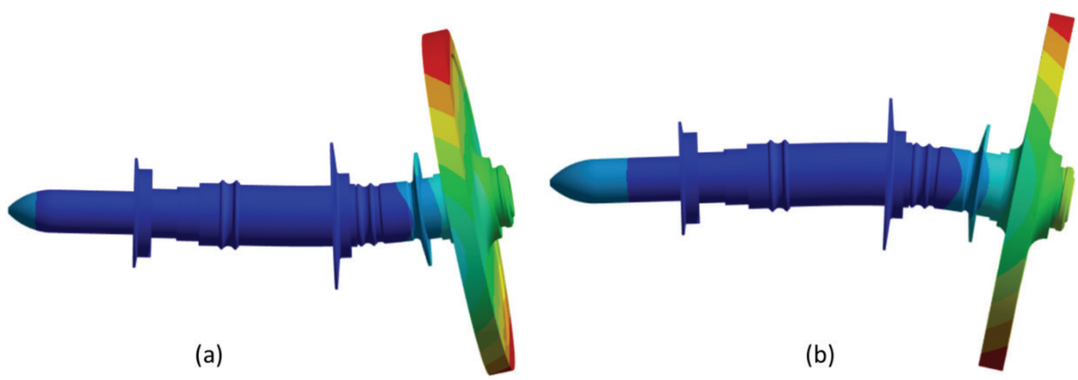

Fig. 4 Rotor Mode Shapes at 5,000 RPM: a) 1st Backward Whirl Bending (203.6 Hz), b) 1st Forward Whirl Bending (306.39 Hz).

Superelement Generation

The whole stator was meshed by using SOLID187 (tet10) elements except for bearing outer races where SOLID185 (hex8) elements were used. The whole model has 865,000 nodes and 481,000 elements. All the interfaces were modeled with Surf-to-Surf Always Bonded Contacts. Inconel 718, with a density of 8240 kg/m^3, a Young's modulus of 200 GPa, and a Poisson's ratio of 0.3, was assigned to all components. The model was fixed by using the indicated locations illustrated in Figure 5.

A condensed model was created for the structural parts depicted in Figure 5. Fixity nodes and interface nodes of the bearing outer race were identified as master nodes. CMS algorithm was employed during condensation. Prior to this, modal analysis was performed to determine how many modes were required. It is aimed to capture approximately 95% of the total mass in all translational directions. The modal analysis indicated that the first 50 modes were necessary to achieve this. Sparse solver was used and expansion pass was disabled. With these options, the run time to generate a condensed model was approximately 7 sec with Distributed Solver using 10 processors.

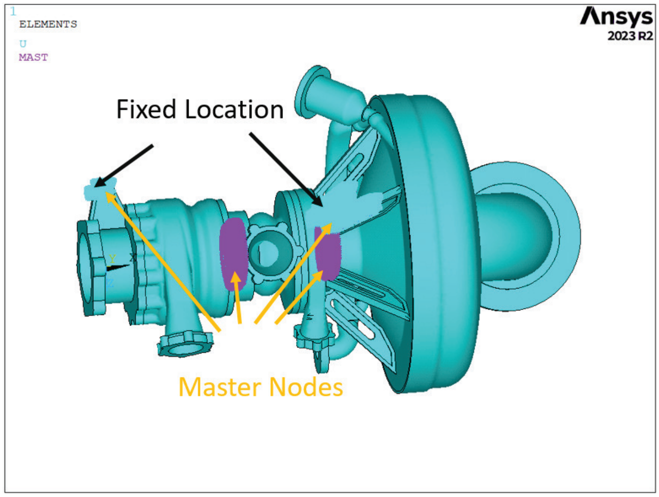

Fig. 5 Turbopump Stator Model for Component Mode Synthesis.

Rotordynamic Model including Stator Flexibility

In this section, the full 3D rotor model was coupled with the superelement representing the stator model. This coupling was facilitated by two bearings with constant stiffness, as shown in Figure 6. To analyze the dynamic behavior of this reduced model, a complex eigenvalue analysis was performed, generating the Campbell diagram for a range of rotor speeds from 5,000 to 30,000 RPM, as shown in Figure 7. Within this diagram, the 1X line represents the rotor's operating speed. Additionally, Figure 8 presents the first backward and first forward mode shapes of the reduced system at a speed of 5,000 RPM, providing valuable insights into the rotor's dynamic performance under these operating conditions.

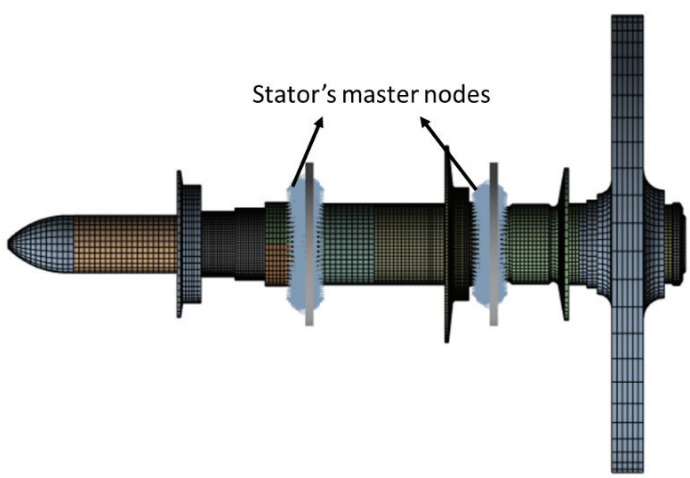

Fig. 6 Coupling between the Rotor and the Superelement (Reduced Model).

As illustrated in Figure 8, the inclusion of stator flexibility leads to a reduction in both the forward and backward whirl speeds. Specifically, the flexibility of the casing decreases the first forward whirl critical speed to 21,000 RPM, representing a reduction of 31% compared to the model that considers only the rotor. This highlights the significant impact that stator flexibility has on the dynamic behavior of the system. Furthermore, the flexibility of the stator introduces a critical speed within a range of approximately $\pm 15\%$ of the operating speed.

To validate the rotordynamic analysis of the reduced system, the complete turbopump model was analyzed by coupling the 3D rotor and stator models, which were prepared for the superelement extraction process, as shown in Figure 9. The rotor and stator were connected using bearing elements with a constant stiffness of 10^8 N/mm. The whole turbopump

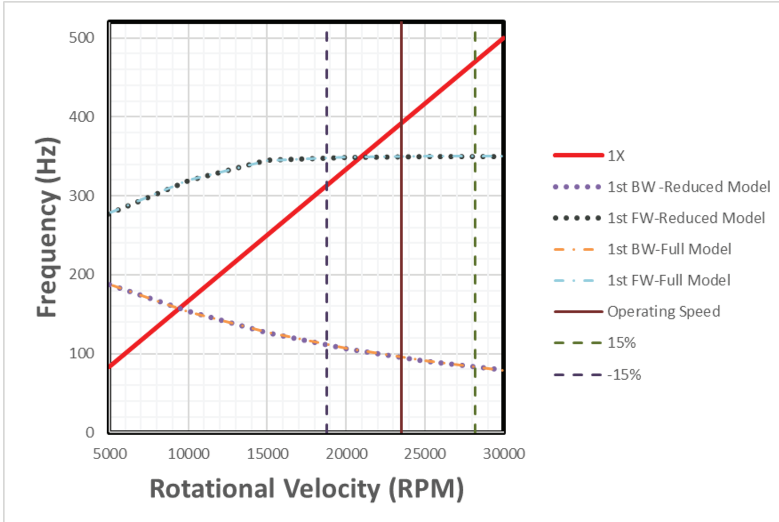

Fig. 7 Campbell Diagram of the Turbopump Rotor with Stator Configuration.

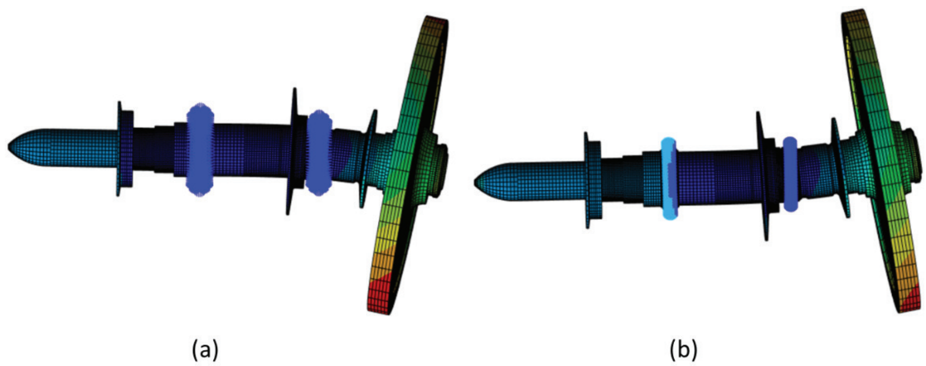

Fig. 8 Reduced Model Rotor Mode Shapes at 5000 RPM: a) First Backward Whirl Bending (187.64 Hz), b) First Forward Whirl Bending (277.85 Hz).

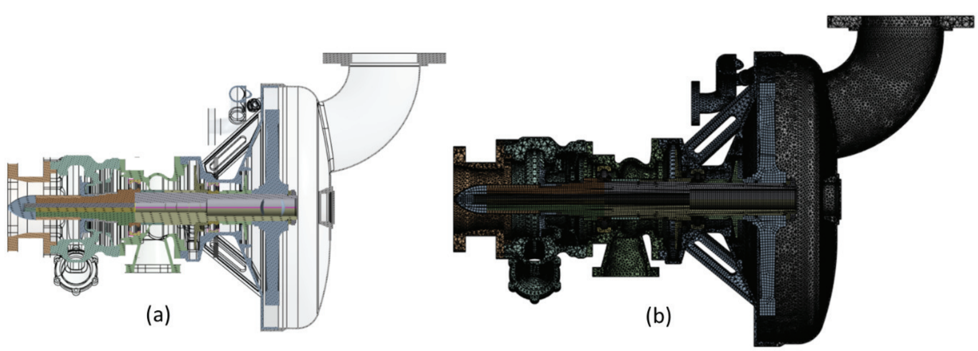

Fig. 9 Whole Turbopump Model a) Geometric Representation b) Finite Element Model Representation.

model consists of 1,001,832 nodes and 572,060 elements, as shown in Figure 9. The stator was predominantly meshed with SOLID187 elements, while the rotor was modeled using SOLID185 elements in ANSYS, ensuring an accurate representation of the system's dynamic behavior. A complex eigenvalue analysis was carried out to develop the Campbell diagram for rotor speeds ranging from 5,000 to 30,000 RPM, as shown in Figure 7. In this diagram, the 1X line indicates the rotor's operating speed, serving as a reference for evaluating resonance conditions. Furthermore, Figure 10 illustrates the first backward and forward mode shapes of the rotor at an operational speed of 5,000 RPM.

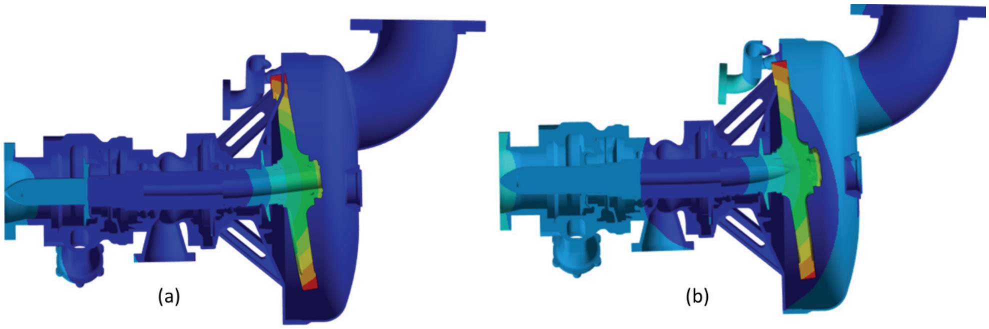

Fig. 10 Mode Shapes of the Whole Turbopump at 5,000 RPM a) First Backward Whirl Bending (187.64 Hz), b) First Forward Whirl Bending (277.85 Hz).

An examination of the Campbell diagram presented in Figure 11 reveals that the critical speeds for the whole turbopump model and the reduced turbopump model are nearly identical. When comparing critical speeds within the 5,000 to 30,000 RPM range, the discrepancy between the two models is less than 0.01%. However, when comparing these results to the rotor-only model, a significant difference of 31% in critical speeds is observed. Furthermore, the Campbell Diagram in Figure 11 indicates that, in the rotor-only model, no critical speed is present within $\pm15\%$ of the operating speed. In contrast, the inclusion of stator flexibility results in a critical speed appearing within this range. These findings underscore the necessity of incorporating stator flexibility in turbopump rotordynamic analyses to ensure accurate results.

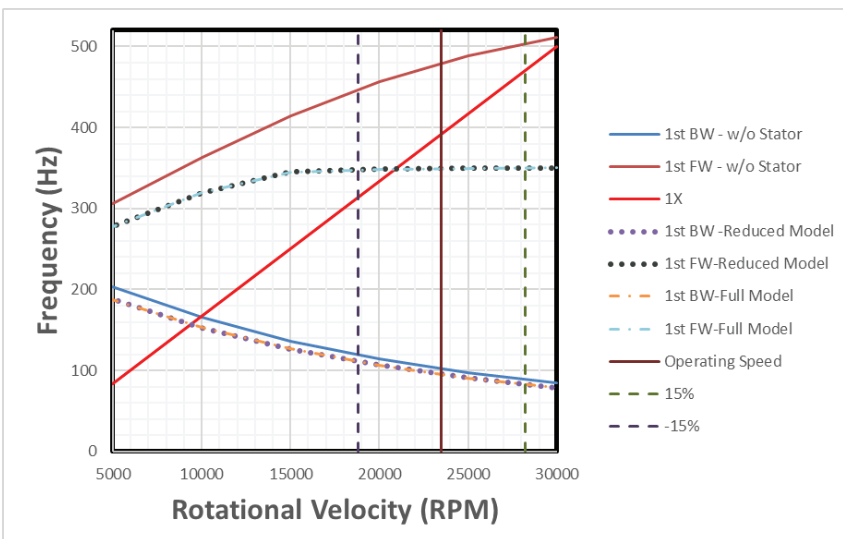

Fig. 11 Campbell Diagram of the Turbopump Rotor.

Wall time refers to the real-time duration required to complete a simulation, measured from start to finish. It encompasses the entire computational process, including overhead tasks such as input data loading, performing calculations, and outputting results. As per Table 1, although the whole turbopump model and reduced model yield almost the same result, the wall time for the reduced model is ten times faster than the whole turbopump model's wall time. Reduced model saves an enormous amount of time while maintaining accuracy. It is important to note that a superelement generation needs to be created only once and can be reused in any subsequent analyses.

Table 1 Wall Time Comparison for Campbell Diagram Generation

Model Name	Wall Time
Rotor without Stator	18 min
Reduced Model	26 min
Whole Turbopump Model	273 min

Conclusion

The use of the superelement approach in this study has proven to be highly effective in reducing the computational effort required for comprehensive rotordynamic analysis of turbopumps. The results of the reduced model closely align with those of the full 3D model, with a minimal discrepancy in critical speeds, thus validating the accuracy of the superelement method. The inclusion of stator flexibility was shown to have a significant impact on the system's dynamic behavior, particularly by lowering the critical speeds of both forward and backward whirl modes. This finding emphasizes the importance of considering stator flexibility in turbopump design to avoid potential resonance issues. The reduction in computation time by an order of magnitude demonstrates the practical advantage of the superelement method, making it an invaluable tool for the design and optimization of rotating machinery in aerospace applications.

References

1. S. DUNKERLY, "On the whirling and vibration of shafts", Phil. Trans. A., 27, p. 249, 1894.
2. Keith E. Rouch, Tim H. McMains, Robert W. Stephenson, Mark F. Emerick, Modeling of complex rotor systems by combining rotor and substructure models, Finite Elements in Analysis and Design, Volume 10, Issue 1, 1991, Pages 89–100, https://doi.org/10.1016/0168-874X(91)90030-3.
3. G. Giancarlo, Dynamics of Rotating Systems, 2005
4. Geradin, M., and N. Kill. "A new approach to finite element modelling of flexible rotors." Engineering Computations: International Journal for Computer-Aided Engineering and Software 1.1 (1984): 52–64.
5. Vollan, Arne & Komzsik, Louis. (2012). Computational Techniques of Rotor Dynamics with the Finite Element Method. 10.1201/b11765.
6. Kumar, Devesh & Juethner, Konrad & Fournier, Yves. (2017). Efficient Rotordynamic Analysis Using the Superelement Approach for an Aircraft Engine. 10.1115/GT2017-64954.
7. Kim, K., & Noah, S. T. (2003). Modal reduction for nonlinear analysis of turbocharger rotors using component mode synthesis. Journal of Vibration and Control, 9(11), 1219–1241. https://doi.org/10.1177/107754603030719
8. Lund, J. W. (1987). Application of modal analysis to rotordynamics. Journal of Engineering for Gas Turbines and Power, 109(1), 13–21. https://doi.org/10.1115/1.3240015
9. Ehrich, F. F. (1999). High-speed rotor dynamics and computational techniques. International Journal of Rotating Machinery, 5(4), 239–251.
10. Gupta, V., Singh, S. P., & Agrawal, V. K. (2015). Nonlinear rotordynamics using component mode synthesis. Journal of Sound and Vibration, 343, 378–392. https://doi.org/10.1016/j.jsv.2015.02.014
11. "ANSYS Mechanical 2024 R2 Substructuring Analysis Guide," 2024.
12. R. R. Craig and C. C. Bampton, "Coupling of Substructures for Dynamic Analyses," *AIAA Journal*, vol. 6, no. 7, 1968, doi: 10.2514/3.4741ï.
13. "Mechanical APDL 2024 R2 Theory Reference."